AD-A073 638   SYRACUSE UNIV N Y DEPT OF ELECTRICAL ENGINEERING   F/G 11/4
MEASUREMENT OF THE ELECTRICAL PROPERTIES OF COMPOSITE MATERIALS--ETC(U)
AUG 79 W J GAJDA   F30602-75-C-0121
UNCLASSIFIED   RADC-TR-79-203   NL

| OF |
AD
A073638

END
DATE
FILMED
10-79
DDC

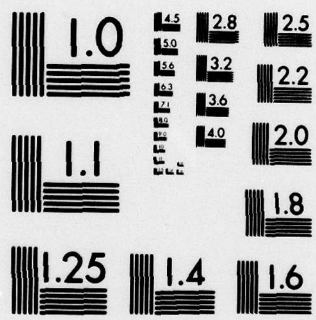
1.0
4.5
5.0
5.6
6.3
7.1
8.0
2.8
3.2
3.6
4.0
2.5
2.2
2.0
1.1
1.8
1.25
1.4
1.6

(12) LEVEL II

RADC-TR-79-208
Phase Report
August 1979

MEASUREMENT OF THE ELECTRICAL PROPERTIES OF COMPOSITE MATERIALS IN THE FREQUENCY RANGE OF DC TO 30 MHz

Syracuse University

W. J. Gajda

ROME AIR DEVELOPMENT CENTER
Air Force Systems Command
Griffiss Air Force Base, New York 13441

[illegible]

This report has been reviewed by the RADC Information Office (OI) and is releasable to the National Technical Information Service (NTIS). At NTIS it will be releasable to the general public, including foreign nations.

RADC-TR-79-203 has been reviewed and is approved for publication.

APPROVED:

ROY F. STRATTON
Project Engineer

APPROVED:

DAVID C. LUKE, Lt Col, USAF
Chief, Reliability & Compatibility Division

FOR THE COMMANDER:

JOHN P. HUSS
Acting Chief, Plans Office

If your address has changed or if you wish to be removed from the RADC mailing list, or if the addressee is no longer employed by your organization, please notify RADC ([illegible]), Griffiss AFB NY 13441. This will assist us in maintaining a current mailing list.

Do not return this copy. Retain or destroy.

UNCLASSIFIED

SECURITY CLASSIFICATION OF THIS PAGE (When Data Entered)

REPORT DOCUMENTATION PAGE		READ INSTRUCTIONS BEFORE COMPLETING FORM
1. REPORT NUMBER: RADC-TR-79-203	2. GOVT ACCESSION NO.	3. RECIPIENT'S CATALOG NUMBER
4. TITLE (and Subtitle): MEASUREMENT OF THE ELECTRICAL PROPERTIES OF COMPOSITE MATERIALS IN THE FREQUENCY RANGE OF DC TO 30 MHz		5. TYPE OF REPORT & PERIOD COVERED: Phase Report, 1 Oct 77 — 30 Sep 78
		6. PERFORMING ORG. REPORT NUMBER: N/A
7. AUTHOR(s): W. J. Gajda, University of Notre Dame		8. CONTRACT OR GRANT NUMBER(s): F30602-75-C-0121, F30602-78-C-0083
9. PERFORMING ORGANIZATION NAME AND ADDRESS: Syracuse University, Syracuse NY 13210		10. PROGRAM ELEMENT, PROJECT, TASK AREA & WORK UNIT NUMBERS: 62702F, 233803P3
11. CONTROLLING OFFICE NAME AND ADDRESS: Rome Air Development Center (RBCT), Griffiss AFB NY 13441		12. REPORT DATE: August 1979
		13. NUMBER OF PAGES: 44
14. MONITORING AGENCY NAME & ADDRESS (if different from Controlling Office): Same		15. SECURITY CLASS. (of this report): UNCLASSIFIED
		15a. DECLASSIFICATION/DOWNGRADING SCHEDULE: N/A

16. DISTRIBUTION STATEMENT (of this Report)

Approved for public release; distribution unlimited.

17. DISTRIBUTION STATEMENT (of the abstract entered in Block 20, if different from Report)

Same

18. SUPPLEMENTARY NOTES

RADC Project Engineer: Roy Stratton (RBCT)

19. KEY WORDS (Continue on reverse side if necessary and identify by block number)

Electromagnetic Compatibility
Composite Materials
Conductivity
Permittivity
Permeability
Graphite/Epoxy
Boron/Epoxy

20. ABSTRACT (Continue on reverse side if necessary and identify by block number)

Work reported here is an extension of work reported in RADC-TR-78-156. A much higher conductivity for boron/epoxy is reported using better contacting techniques. For graphite/epoxy: coupled circuit theory is used to relate the conductivity to the measured resistance of a sample; the effect of absorbed moisture on the conductivity is report, and the effective conductivity of a multiply laminate is reexamined.

DD FORM 1 JAN 73 1473

UNCLASSIFIED

SECURITY CLASSIFICATION OF THIS PAGE (When Data Entered)

339 712

PREFACE

This effort was conducted by Notre Dame University subcontracting through Syracuse University under the sponsorship of the Rome Air Development Center Post-Doctoral Program for Rome Air Development Center. Dr. Roy F. Stratton, RADC/RBCT, was project engineer and provided overall technical direction and guidance.

The RADC Post-Doctoral Program is a cooperative venture between RADC and some sixty-five universities eligible to participate in the program. Syracuse University (Department of Electrical Engineering), Purdue University (School of Electrical Engineering), Georgia Institute of Technology (School of Electrical Engineering), and State University of New York at Buffalo (Department of Electrical Engineering) act as prime contractor schools with other schools participating via sub-contracts with prime schools. The U.S. Air Force Academy (Department of Electrical Engineering), Air Force Institute of Technology (Department of Electrical Engineering), and the Naval Post Graduate School (Department of Electrical Engineering) also participate in the program.

The Post-Doctoral Program provides an opportunity for faculty at participating universities to spend up to one year full time on exploratory development and problem-solving efforts with the post-doctorals splitting their time between the customer location and their educational institutions. The program is totally customer-funded with current projects being undertaken for Rome Air Development Center (RADC), Space and Missile Systems Organization (SAMSO), Aeronautical System Division (ASD), Electronic Systems Division (ESD), Air Force Avionics Laboratory (AFAL), Foreign Technology Division (FTD), Air Force Weapons Laboratory (AFWL), Armament Development and Test Center (ADTC), Air Force Communications Service (AFCS), Aerospace Defense Command (ADC), Hq USAF, Defense Communications Agency (DCA), Navy, Army, Aerospace Medical Division (AMD), and Federal Aviation Administration (FAA).

Further information about the RADC Post-Doctoral Program can be obtained from Mr. Jacob Scherer, RADC/RBC, Griffiss AFB, NY, 13441, telephone Autovon 587-2543, Commercial (315) 330-2543.

TABLE OF CONTENTS

LIST OF ILLUSTRATIONS

LIST OF TABLES

1) INTRODUCTION

This report describes procedures and results involving the measurement and modeling of the intrinsic electrical parameters of advanced composite materials over the frequency range from DC to 50 MHz. The primary focus of the work has been the electrical conductivity. This work was carried out from October 1, 1977 to September 30, 1978 in the Department of Electrical Engineering at the University of Notre Dame.

The details of the measurement procedures used are unchanged from earlier work[1]. As a brief summary of previous results, it should be mentioned that the three composite materials of interest (graphite/epoxy, boron/epoxy and Kevlar/epoxy) are all weakly diamagnetic with magnetic susceptibilities on the order of -10^{-7}. The low frequency permeabilities of these materials are essentially equal to that of free space. Permeability measurements were made by determining sample weight change as a function of magnetic field at DC and 60 Hz. Permeabilities were also measured at 100 Hz using a vibrating sample magnetometer.

Permittivities of representative samples of boron/epoxy and Kevlar/epoxy were determined by measuring the capacitance of rectangular slabs using bridges over the frequency range of 10 kHz to 50 MHz. The relative permittivities were 5.6 for boron/epoxy and in the range of 3.6 - 5.8 for Kevlar/epoxy.

A similar approach with graphite/epoxy failed to produce meaningful results because of the relatively large conductivity associated with these samples. Their impedances were essentially resistive even at 50 MHz. It was concluded that the permittivity of graphite/epoxy is indeterminant over the frequency band investigated.

Sample conductances were measured using two-point techniques in which a known current was injected across one face of a rectangular sample and extracted from the opposite face.

For graphite/epoxy, DC conductivities ranged from 10 to $2(10^4)$ mhos/m. while boron/epoxy displayed conductivities from $9(10^{-8})$ to $3.3(10^3)$ mhos/m. The larger values are associated with current parallel to fibers in unidirectional samples while the lower values are found when current is orthogonal to the fiber axis. The conductivities of samples composed of multidirectional plies fall between these two bounds.

The conductivity of Kevlar/epoxy was on the order of 10^{-9} mhos/m. and displayed no geometric anisotropy. High field properties of Kevlar/epoxy were examined during the current program.

The effective conductivities of boron/epoxy and Kevlar/epoxy are independent of frequency over the range of interest.

As shown in previous work[1], the measured conductivity of graphite/epoxy composite materials shows an increase with frequency and this effect cannot be completely explained using conventional skin effect theory because of the inhomogeneous nature of the materials themselves as well as the rectangular cross-section of the samples. There is a need to replace the skin effect approximation with a model which explicitly includes the inductive coupling between graphite fibers.

During the current research period, a coupled circuit theory model was analyzed via digital computer and provided an acceptable fit to the frequency variation of the effective conductivity of graphite/epoxy. The basic conclusion is that the intrinsic conductivity is independent of frequency over the range DC to 50 MHz.

A study of the effects of moisture absorption upon the electrical conductivities of advanced composites was completed. Boron/epoxy and Kevlar/epoxy displayed no electrical variation with exposure to moisture. The longitudinal conductivity of unidirectional graphite/epoxy was also unaffected but the transverse conductivity of the same samples decreased although it is likely that this decrease, in operational situations, will be limited to 20% of the dry value.

Finally, a revised model for the calculation of the conductivities of multiple-ply lay-ups is developed in which it is pointed out that the "electrical independence of individual plies" assumption made previously[1] is not always valid.

2) KEVLAR/EPOXY PROPERTIES

Additional samples of Kevlar/epoxy were obtained and measurements made of their conductivity and permittivity using methods described above. Permeability was not measured in view of the earlier finding that the composite materials of interest in this work have essentially a unity relative permeability. The conductivity of these samples of Kevlar/epoxy had a slight dependence on frequency; for example, a value of $2.2(10^{-8})$ mhos/m. at DC and $5(10^{-9})$ mhos/m. at 100 kHz. The frequency dependence is so slight and the conductivities are so small as to allow the conclusion that this material is a good insulator over the frequency range of interest in this report. For this reason, no detailed study of the frequency dependence of the conductivity was carried out since it would appear to be, at best, of only marginal operational interest.

The relative permittivity of the additional samples was 5.85 which is a significant increase over the value (3.6) reported earlier[1]. In view of the simple method used to measure relative permittivities, we conclude that these variations may reflect natural variations in epoxy chemistry. Manufacturers do not reveal changes in epoxy formulation and, as a consequence, some variation is to be expected in the dielectric properties of Kevlar/epoxy although this study has not involved a sufficient statistical sampling to allow a definitive conclusion.

Figure 1 reveals that the electrical conductivity of Kevlar/epoxy is nearly constant for electric fields as large as $1(10^5)$ volts/m. There is no evidence of pre-breakdown behavior over this range of excitations. A least-squares fit to the data shows a slight upward slope but dielectric breakdown does not occur for fields less than $1(10^5)$ volts/meter.

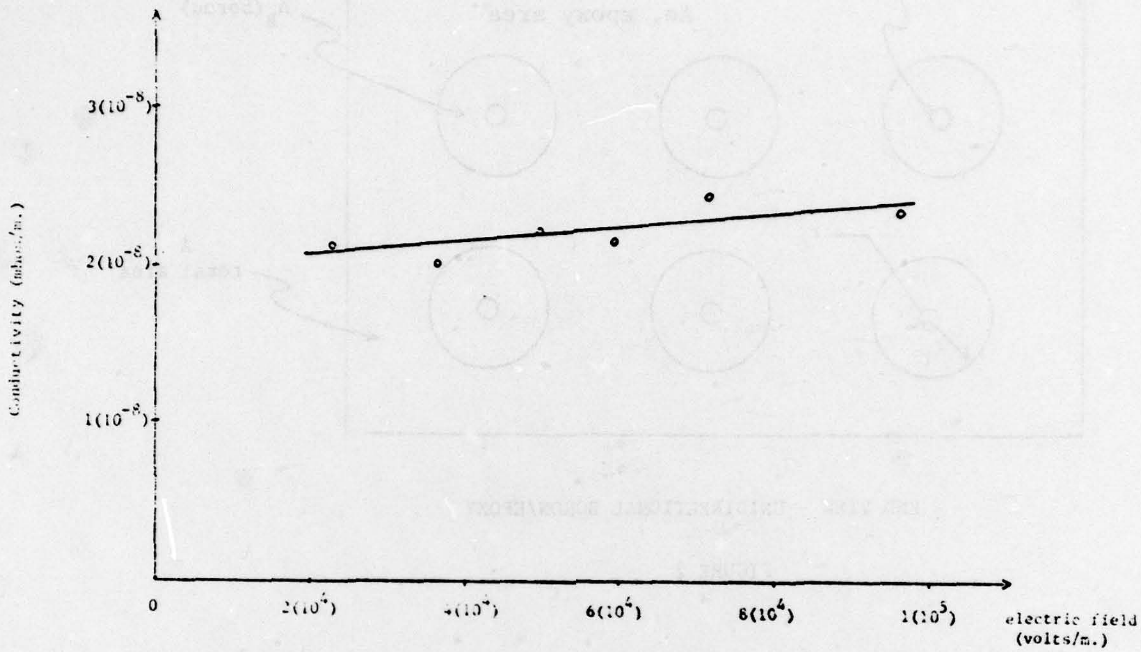

CONDUCTIVITY VS. ELECTRIC FIELD - KEVLAR/EPOXY

FIGURE 1

3) LONGITUDINAL CONDUCTIVITY OF BORON/EPOXY

It had previously been reported[1,2] that the longitudinal conductivity of unidirectional samples of boron/epoxy was in the range of 10 to 100 mhos/m. These values contradict the predictions of a simple model as discussed below.

A simplified end view of a unidirectional boron/epoxy sample is shown in Figure 2, the 'boron' fibers consist of a sheath of boron around an inner core which was tungsten when the boron growth began but converts to a mixture of boron tungstides during the chemical vapor deposition of boron. It is evident that the overall conductance of the boron/epoxy will be the sum of the conductances of the core cylinders, the boron sheaths and the epoxy matrix.

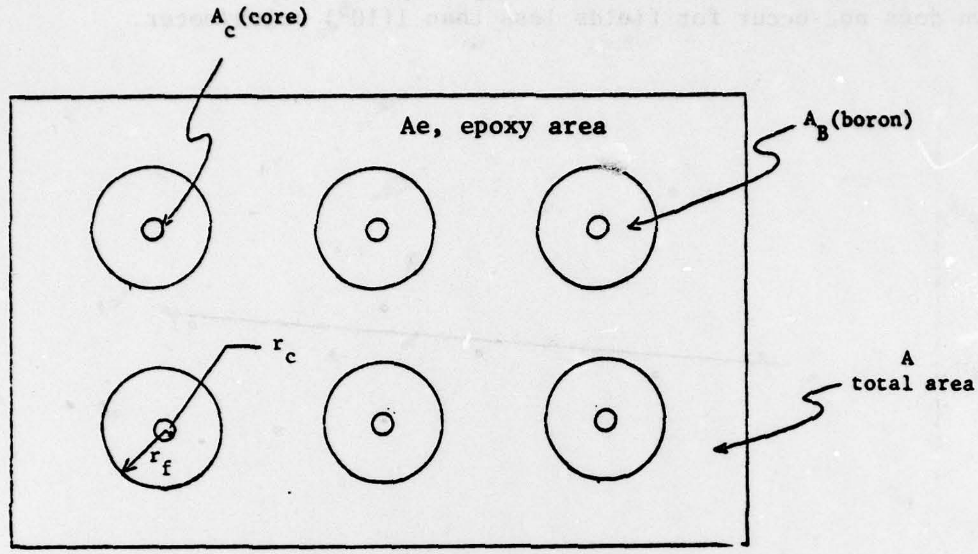

END VIEW - UNIDIRECTIONAL BORON/EPOXY

FIGURE 2

An expression for the conductivity of boron/epoxy may be derived from geometric factors and the conductivities of the three constituents. Let r_f be the radius of a given fiber and r_c the radius of the core. The area A_f of an individual fiber may be written as

$$A_f = \pi r_f^2$$

while A_c , the area of a fiber core, is

$$A_c = \pi r_c^2$$

It is convenient to define a dimensionless parameter η as

$$\eta = \frac{A_f}{A_c} = \left(\frac{r_f}{r_c}\right)^2$$

The total area A_B of boron associated with a single fiber is given by

$$A_B = A_f - A_c$$

If N is the number of fibers in the sample of interest and f is the volume fraction, NA_f/A, it follows that:

$$fA = NA_f = NA_c + NA_B$$

but

$$A_f = \eta A_c \quad \text{and}$$

$$A_B = A_f - A_c = (\eta - 1)\, A_c$$

The geometry is indicated in Figure 3. Note that A is the total cross-sectional area and L is the sample length.

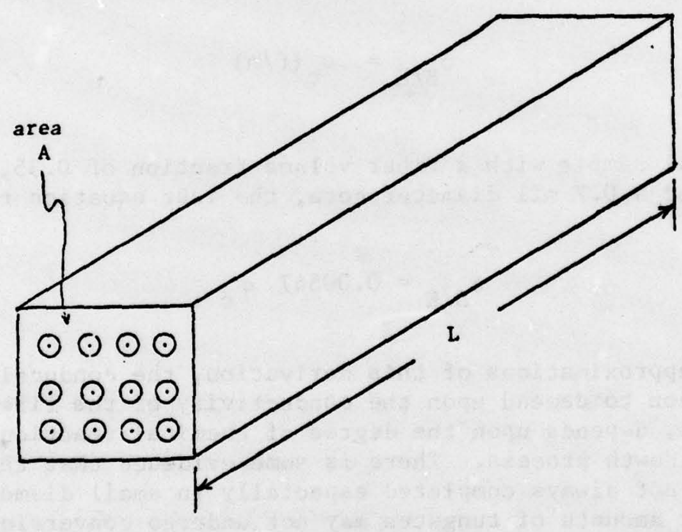

BORON/EPOXY SAMPLE GEOMETRY

FIGURE 3

The total conductance $G_{B/E}$ ma. be written as the conductances of the three constituents of the sample.

$$G_{B/E} = \frac{\sigma_e A_e}{L} + \frac{\sigma_B N A_B}{L} + \frac{\sigma_c N A_c}{L}$$

where σ_e, σ_B, σ_C are the conductivities of the epoxy, boron and core respectively.

An effective boron/epoxy conductivity $\sigma_{B/E}$ is defined as

$$G_{B/E} = \frac{\sigma_{B/E} A}{L}$$

Combining the equations above yields

$$\sigma_{B/E} = \sigma_e(1-f) + \sigma_B \frac{\eta-1}{\eta} f + \sigma_c \frac{f}{\eta}$$

It has been found experimentally[3] that the conductivities of both boron and epoxy are orders of magnitude less than the conductivity of the core which implies that the boron/epoxy conductivity may be approximated as

$$\sigma_{B/E} = \sigma_c (f/\eta)$$

For a typical sample with a fiber volume fraction of 0.35, a 5.6 mil diameter fiber and a 0.7 mil diameter core, the last equation reduces to

$$\sigma_{B/E} = 0.00547 \ \sigma_c$$

Within the approximations of this derivation, the conductivity of boron/epoxy is seen to depend upon the conductivity of the fiber core and this, in turn, depends upon the degree of chemical reaction it undergoes during the growth process. There is some evidence that the conversion reaction is not always completed especially in small diameter fibers where significant amounts of tungsten may not undergo conversion. Despite this, we are in a position to place bounds upon the conductivity of boron/epoxy. If the core were totally unconverted, i.e., it remained pure tungsten, the conductivity of boron/epoxy would be

$$\sigma_{B/E} = 0.00547 \ \sigma_{tungsten} = (0.00547)(1.8)(10^7)\text{mhos/m.}$$
$$= 9.9\ (10^4)\ \text{mhos/m.}$$

If the core were totally converted to W_2B_5 , the composite conductivity would be

$$\sigma_{B/E} = 0.0547\ \sigma_{W_2B_5} = (0.00547)(3)(10^5)\ \text{mhos/m.}$$

$$= 1.64\ (10^3)\ \text{mhos/m.}$$

It should be mentioned that the core conversion kinetics are poorly understoody and it is possible, in some samples, that the core converts to a material with a lower conductivity than W_2B_5 . The value of boron/epoxy conductivity obtained assuming a pure tungsten core represents an upper bound on the conductivity of boron/epoxy (within the limitations of this model) but the value obtained assuming a core totally converted to W_2B_5 does not necessarily represent a lower bound.

In preliminary experiments[1], a value of 30 mhos/m. was reported for longitudinal charge motion in unidirectional samples of boron/epoxy. Once the predictions of the above model were determined, it became clear that the experimental measurements may have been clouded by relatively high resistance contacts. To circumvent this problem, care was taken to plate thin nickel layers onto the edges of carefully abraded edges of boron/epoxy[3]. Four samples of Avco Rigidite 5505 boron/epoxy were cured to a nominal fiber volume fraction of 0.35 and the measured values of conductivity are shown in Table I below.

Sample	Number of Plies	$\sigma_{B/E}$ (mhos/m.)
#2	20	1110
#5	2	3300
#8	5	1400
#9	17	1400

Table I - Boron/Epoxy Conductivity Data

These values cluster reasonably well around the value derived above assuming complete conversion to W_2B_5 . Rather than the values of 10 to 100 mhos/m. commonly cited in the literature, the above results indicate that the intrinsic longitudinal conductivity of boron/epoxy is on the order of 1000 mhos/m. However, the detailed experimental procedures for obtaining these values clearly indicate that it is not simple to make good, low-resistance electrical contacts to this material. It is likely that the poor shielding characteristics of boron/epoxy reported by many investigators[2,4] are more a measure of the difficulty in avoiding inadvertent field penetration through the sample edges due to inadequate electrical contact than of the low intrinsic conductivity of boron/epoxy.

4) *COUPLED CIRCUIT THEORY*

Coupled circuit theory can be applied to composite materials by considering a given sample to consist of a finite number of finite length conductors arranged in parallel as sketched in Figure 4. This represents the so-called longitudinal sample geometry which was investigated in detail last year[1]. Each of the conductors in this model has the same length and the same resistance. The resistance of each conductor is that of a single graphite fiber. We use the values obtained previously[3] for the resistance of the individual fibers.

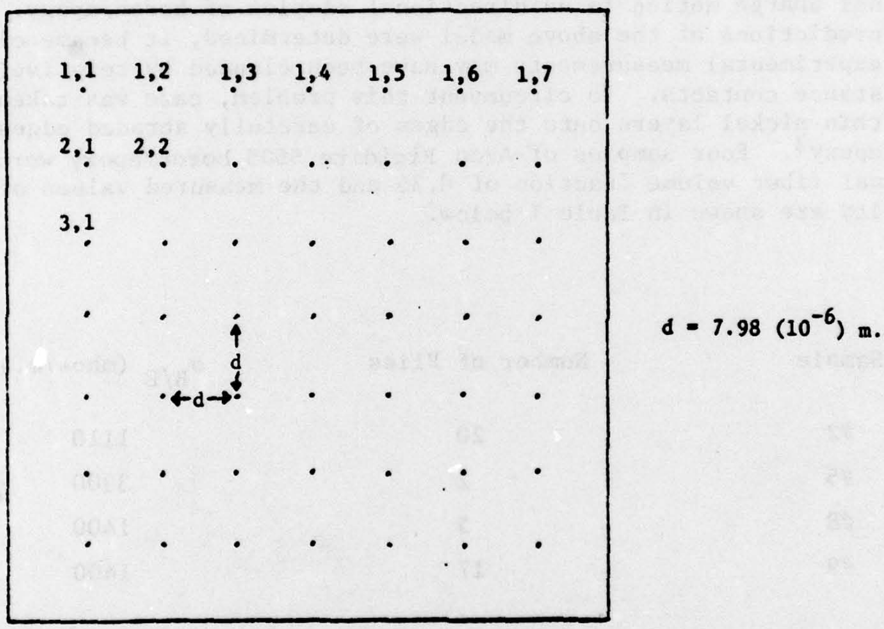

UNIDIRECTIONAL GRAPHITE/EPOXY FIBER INDEXING

FIGURE 4

For ease of comparison with experimental results, the length of the sample was taken to be 0.082 meters and the resistance of a single fiber was set equal to 214,000 ohms. Using known values for the volume fractions of cured graphite/epoxy samples, the average distance between the fibers was found to be 7.98 (10^{-6}) meters as shown in Figure 4.

In order to reduce computational complexity in developing a suitable coupled circuit theory, each fiber was assumed to be infinitesimally thin and spaced by the distance cited in the above paragraph. Once the geometry of the sample was determined, the mutual inductance between each pair of fibers was determined using Neumanns' Formula[5].

$$M_{n,m} = \frac{\mu}{4\pi} \int_0^L \int_0^L \frac{d\underset{\sim}{n} \cdot d\underset{\sim}{m}}{r}$$

where $M_{n,m}$ is the mutual inductance between the n^{th} and m^{th} fibers,

μ = 4π (10^{-7}) henries/meter, (the permeability of epoxy),

L = fiber length (meters),

dn,dm = vector length elements along the fibers and

r = distance between $d\underset{\sim}{n}$ and $d\underset{\sim}{m}$ (meters).

This integral may be solved directly[6] for the case of two parallel fibers with the result that

$$M_{n,m} = \frac{\mu}{2\pi} [L \ln((L + \sqrt{L^2+d^2})/d) - \sqrt{L^2+d^2} + d]$$

where d is the center-to-center distance between the fibers. It should be noted that the factor μ was omitted in reference 6.

Following Graneau, a set of coefficients can be calculated which are used to form a power series expansion in frequency for the current i_n in each fiber

$$i_n = \sum_{r=1}^{\infty} (-1)^{r-1} C_r \frac{d^{r-1} e}{dt^{r-1}}$$

where e is the excitation voltage and

$$C_1 = R_n^{-1}$$

$$C_2 = R_n^{-1} \sum_m \frac{M_{n,m}}{R_m}$$

$$C_3 = R_n^{-1} \sum_m \frac{M_{n,m}}{R_m} \sum_\ell \frac{M_{\ell,m}}{R}$$

$$\vdots$$

where R_n is the resistance of the n^{th} fiber.

Upon examination, it is found that the above equation for the current i_n states that a current flowing in the n^{th} fiber induces currents in all the other fibers and these in turn modify the current in fiber n which in turn causes a change in the currents in all the other fibers and so forth. The sum of all the induced currents is i_n. If we assume sinusoidal excitation, the above equation reduces to the form used in our computer simulation.

Using sinusoidal steady state notation, we write

$$e = E\, e^{j\omega t}, \qquad i_n = I_n\, e^{j\omega t}; \quad \text{then}$$

$$I_n = E(C_1 - C_3\, \omega^2 + C_5\, \omega^4 - \ldots) + j\, E(-C_2 \omega + C_4\, \omega^3 - C_6\, \omega^5 + \ldots)$$

A simple algorithm may be used to generate the needed coefficients C_n. First, an array is constructed which contains all of the mutual inductance coefficients.

	1	2	3	m. . . .	g	(A)	(B)	(C)
1	0	$M_{1,2}$	$M_{1,3}$	. . $M_{1,m}$	. . $M_{1,g}$	$R_f^2 C_2$	$R_f^3 C_3$	$R_f^4 C_4$
2	$M_{2,1}$	0	$M_{2,3}$	. . $M_{2,m}$	. . $M_{2,g}$	---	---	---
3	.	.	.	.	.	.	.	.
.	.	.	.	.	.	.	.	.
.	.	.	.	.	.	.	.	.
n	$M_{n,1}$	.	. . .	$M_{n,m}$	. . $M_{n,g}$	---	---	---
.	.	.	.	.	.	.	.	.
.	.	.	.	.	.	.	.	.
.	.	.	.	.	.	.	.	.
g	$M_{g,1}$	.	. . .	$M_{g,m}$	. . . 0	---	---	---
.	.	.	.	.	.	.	.	.
.	.	.	.	.	.	.	.	.
.	.	.	.	.	.	.	.	.
a	--- . . .	. . .	. . .	--- . . .	---	.	.	.

All of the elements of the first row are summed and placed on the appropriate line in Column A. This is the quantity $R_f^2C_2$ for the first fiber, where R_f symbolizes the resistance of this fiber. This procedure is repeated for each row to obtain a value of $R_f^2C_2$ for each fiber. We assume that R_f is identical for each fiber. Next, all of the elements in Column 1 are added and the sum is placed on the appropriate line in row a . This procedure is repeated for all of the columns. Now, each matrix element is multiplied by the number at the bottom of its column in row a . The products in each row are then added and the resultant sum placed in column B. The values resulting in column B are those of $R_f^3C_3$ for each fiber. A similar procedure is used to find values of $R_f^4C_4$. In this way, the expansion coefficients C_1, C_2, C_3, C_4 ... are determined to allow evaluation of the current.

Although this procedure is cumbersome to describe in words, it provides a relatively straightforward way to calculate values for the needed coefficients. The detailed calculations of these coefficients were carried out using a digital computer as described below.

Two computer programs were written, debugged and used to calculate current distribution in longitudinal samples of advanced composite materials. The first gave exact results in accordance with coupled circuit theory but consumed large amounts of computer time and memory and could only be implemented for relatively small samples. The maximum possible sample was a square with 48 fibers along each side (i.e., a total of 2304 fibers). The second program involved approximations to be described below and could be used for samples virtually unlimited in size. It should be noted here that the second program gave results essentially identical to the first program when identical samples were analyzed. As presently written, the programs require samples of square cross-section but they may be easily modified for more general rectangular shapes.

The details of the programs are provided in Appendix A. In the discussion to follow, the exact version will be called Program I and the approximation Program II.

A thorough comparison of the theoretical predictions of coupled circuit theory and the available experimental data is not possible here in view of the late completion date of the theoretical model. As a consequence, we have limited the comparison to experimental results for the sample described in Table II. The impedance of this sample was measured, for various frequencies, using a circuit which had been found in earlier work[1] to produce accurate data over the frequency range DC to 50 MHz. Measurements on this sample were taken several different times, over a period of weeks, and were found to be reproducible. There were no problems with contact degradation.

TABLE II

Frequency Response Six Ply Unidirectional Graphite/Epoxy Sample

R_{DC} = 3.76 ohms Width = 1.79 mm

Thickness = 2.04 mm. Length = 82 mm

Number of fibers = 239 x 210

Cross-Section aspect ratio = 1.14

f(MHz)	$\|Z(\text{ohms})\|$
.5	3.76
1.0	3.76
1.5	3.76
5.0	3.76
10.0	3.76
15.0	6.82
20.0	8.14
25.0	10.24
30.0	12.50
35.0	14.94
40.0	17.57
45.0	18.96
50.0	20.06

In view of the increasing impedance with frequency, the graphite/epoxy sample was modeled as a series resistor-inductor circuit. The resistance was taken to be the DC resistance and the inductance was calculated using the formula

$$L = \sqrt{\frac{Z^2 - R_{DC}^2}{(2\pi f)^2}}$$

where Z is the measured impedance (ohms),
R_{DC} the DC resistance (ohms),
f the frequency (Hertz) and
L the inductance (henries).

The results of these calculations are presented in Table III. Except at very low frequencies, the average value of inductance was $628(10^{-6})$ henries. The maximum deviation from this value over the entire frequency range of interest was 8.9%.

TABLE III

Theoretical Inductance of Sample of Table II

f(MHz)	Calculated Inductance (henries)
.5	0
1.0	0
1.5	0
5.0	0
10.0	0
15.0	$603(10^{-8})$
20.0	$574(10^{-8})$
25.0	$606(10^{-8})$
30.0	$632(10^{-8})$
35.0	$657(10^{-8})$
40.0	$683(10^{-8})$
45.0	$667(10^{-8})$
50.0	$660(10^{-8})$

One of the major results in early studies of skin effect in conductors of any shape was known as the Principle of Similitude[7,8]. This principle states that, for any conductor or group of conductors of the same shape and material, there is a definite value of the resistance ratio R_{AC}/R_{DC} for each value of f/R_{DC} where f is the frequency at which the measurements are made. It should be noted that this statement makes no reference to the relative sizes of the samples. In other words, if one had a sample of a specific cross-section, any other sample of the same cross-section, regardless of the relative sizes, will produce the same curve of R_{AC}/R_{DC} versus f/R_{DC}. This is borne out in the figures published by Dwight[7] and Forbes[8] in which reference is made only to the type of the cross-section and not the size. This principle is, of course, valid for all frequencies.

We used the Principal of Similitude to compare the results obtained from Program II for samples of square cross-section of 68, 84, 100, and 239 fibers on a side. The fiber packing density was assumed to be the same and, as a consequence, each of these four samples had different cross-sectional areas. The results of this comparison are shown in Table IV and Figure 5. There is an exact correlation between the 68, 84 and 100 fibers-on-a-side samples while largest sample shows some deviation which will be explained below. It should be noted that Figure 5 is a plot of

$$R_{AC}/R_{DC} \text{ versus } \sqrt{f/R_{DC}}$$

TABLE IV

Similitude Data for Three Fiber Arrays

	$R_{DC} = 46.4$ 68x68		$R_{DC} = 30.42$ 84x84		$R_{DC} = 3.76$ 239x239	
f(MHz)	$\sqrt{f/R_{DC}}$	R_{AC}/R_{DC}	$\sqrt{f/R_{DC}}$	R_{AC}/R_{DC}	$\sqrt{f/R_{DC}}$	R_{AC}/R_{DC}
5	328	1.002	405	1.004	516	1.005
10	464	1.007	573	1.015	729	1.024
15	568	1.016	702	1.034	893	1.056
20	656	1.028	811	1.059	1030	1.096
25	734	1.045	906	1.091	1150	1.146
30	804	1.062	993	1.129		

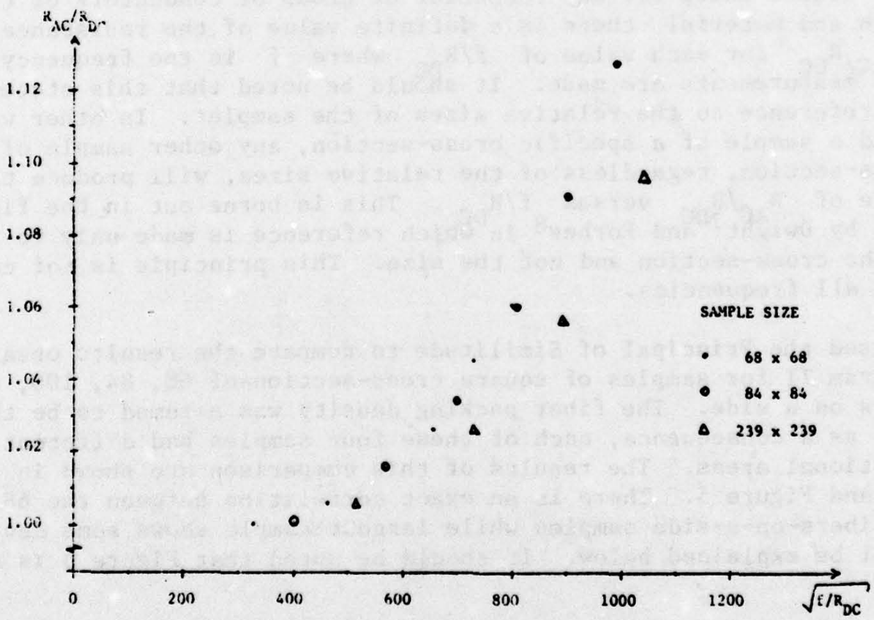

EFFECT OF SAMPLE SIZE ON COUPLED CIRCUIT MODEL

FIGURE 5

An examination of the results produced by Program II reveals that, for the given fiber packing density and square cross-section, the series used to determine the current fails to converge once

$$\sqrt{f/R_{DC}} > 1200.$$

For larger samples, the DC resistance is correspondingly decreased and the series diverges. We conclude that as the size of the theoretical sample increases, the results of the computer program become unreliable at high frequencies and this is manifested as a sudden decrease in resistance. These results are shown in Figure 6.

Since the maximum value of $\sqrt{f/R_{DC}}$ which can be used in the program is 1200 and the maximum value occuring in our laboratory experiments is 2825, there is a rather large frequency gap over which we must extrapolate. However, since the graph of R_{AC}/R_{DC} is known to become linear as f/R_{DC} increases, an attempt at linear extrapolation appears to be valid.

Using this approach yields good agreement with the experimental results as shown in Table V.

TABLE V

Linear Extrapolation of Computer Data

f(MHz)	Extrapolated Theory R_{AC} (ohms)	Experiment R_{AC} (ohms)
15	6.78	6.82
30	12.40	12.50
50	19.32	20.06

We believe that these results demonstrate that coupled circuit theory provides a valuable means of modelling the inductive coupling effects in longitudinal samples of graphite/epoxy composites. Although this is only one special case of the spectrum of composite material and sample geometries of interest, it is important to recognize that it is the only case in which significant frequency dependence of conductivity was observed over a range of DC to 50 MHz. In multiple-ply samples of graphite/epoxy, it is the longitudinal plies which dominate the observed electrical behavior.

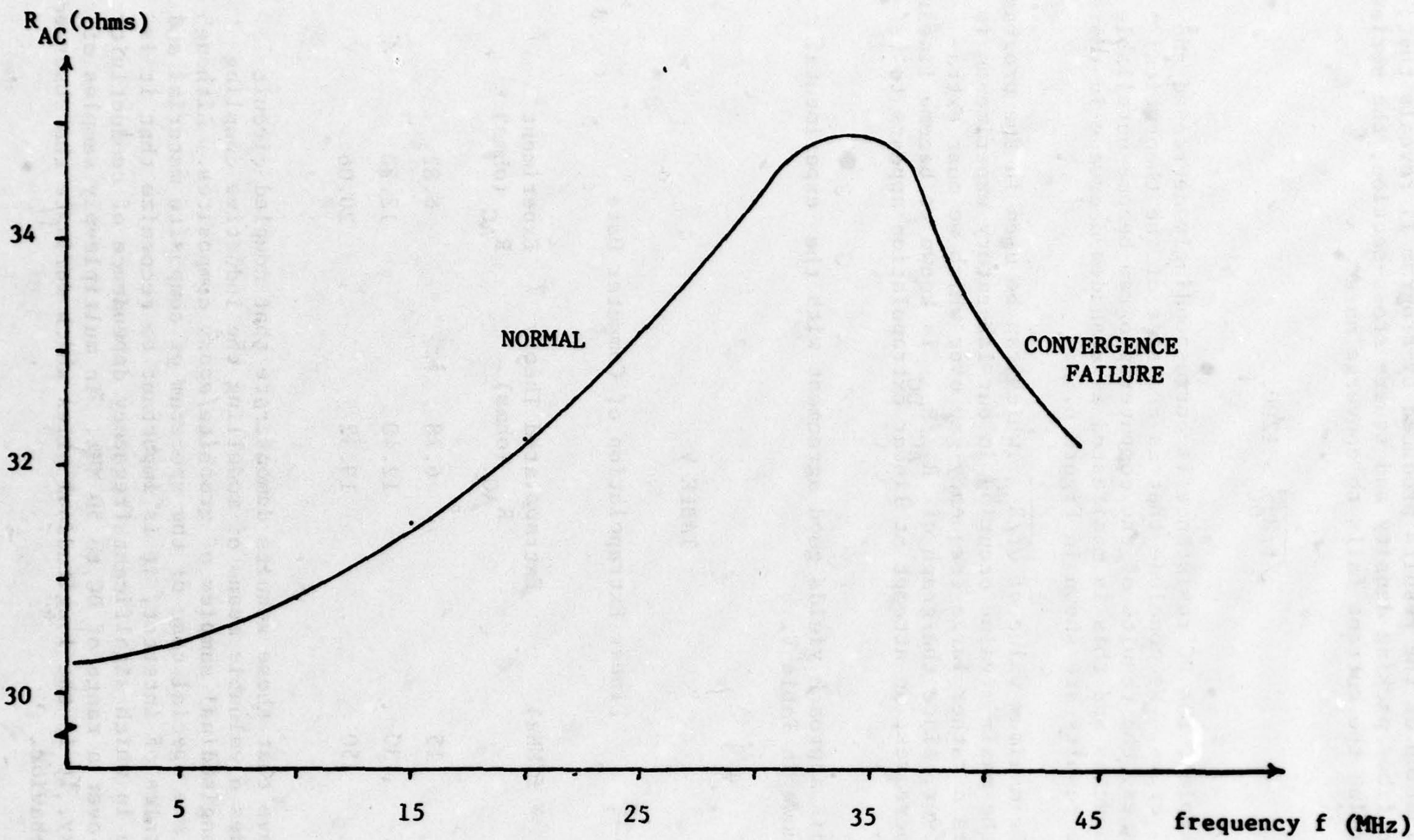

NON-CONVERGENCE OF THE COUPLED CIRCUIT MODEL

FIGURE 6

Coupled circuit theory could, of course, be applied to boron/epoxy but, due to the larger fiber spacing and lower conductivity, no frequency dependent effects would be observed over the frequency range of DC to 50 MHz. This expectation is in agreement with experimental results.

5) EFFECTS OF ABSORBED MOISTURE

The effects of absorbed moisture on the electrical properties of advanced composite materials are of significant interest in view of the anticipated exposure of these materials to high temperatures and high relative humidities. For example, operational experience indicates that aircraft stationed in tropical environments will, over a period of years, absorb as much as 4 weight per-cent of water. The basic mechanism involved is diffusion of water molecules from the surface of a composite panel to the interior. Of course, in any operational situation, the boundary conditions at the surface (that is, the surface moisture concentration) and the temperature will vary with time and detailed numerical calculations of this process using realistic temperature-relative humidity cycles have been carried out[9]. It is anticipated that a moisture content of 4 weight per-cent is the maximum that will be encountered under worst case operational conditions.

Such moisture absorption is important because the mechanism whereby the water enters the composite involves the hygroscopic nature of the epoxy resins used. The epoxies literally swell as they absorb water and this process occurs independently of the existence of the reinforcing fibers. There is, to our knowledge, no evidence to indicate that moisture is absorbed by the reinforcing fibers whether they are graphite, boron or Kevlar. This swelling process has led to decreases in high temperature strengths as great as 40% and, as a consequence, has been of great interest to individuals concerned with mechanical properties. The diffusion process itself has been carefully modelled and a wide range of data is available concerning the rates at which moisture is absorbed into composites at various temperatures from various humidity environments. We repeat none of the theories here but will cite several of the results obtained by other authors[10].

Because we are examining the electrical properties of these materials, it is natural to examine the effects of absorbed moisture on the three advanced composite materials under investigation.

A worst-case "relative humidity" environment was used in that samples were immersed in distilled-deionized water for different times. This procedure insured the maximum absorption of water within the time allowed for a given experiment. The basic procedure was to measure the electrical conductivity of the material, immerse samples for various lengths of time (at a constant 23°C) and measure the resultant sample conductivities. In the beginning, the samples were immersed with the electrical contacts attached and problems occurred in contact degradation. None of the results from these experiments are reported because we are sure that the measured changes in conductivities were more a function of contact change than in the intrinsic conductivity of the materials. To correct this problem, contacts were added after water immersion in all results reported below.

Samples of Kevlar/epoxy and boron/epoxy revealed no change in electrical conductivity for any direction of current. For example, in unidirectional boron/epoxy samples, neither the longitudinal nor the transverse conductivities changed with exposure to water for as long as 40 days.

In the case of graphite/epoxy, only unidirectional samples were examined and significant changes in conductivity were found to occur only for the transverse (current across the fibers) direction. The data is plotted in Figure 7. A marked decrease in transverse conductivity is evident.

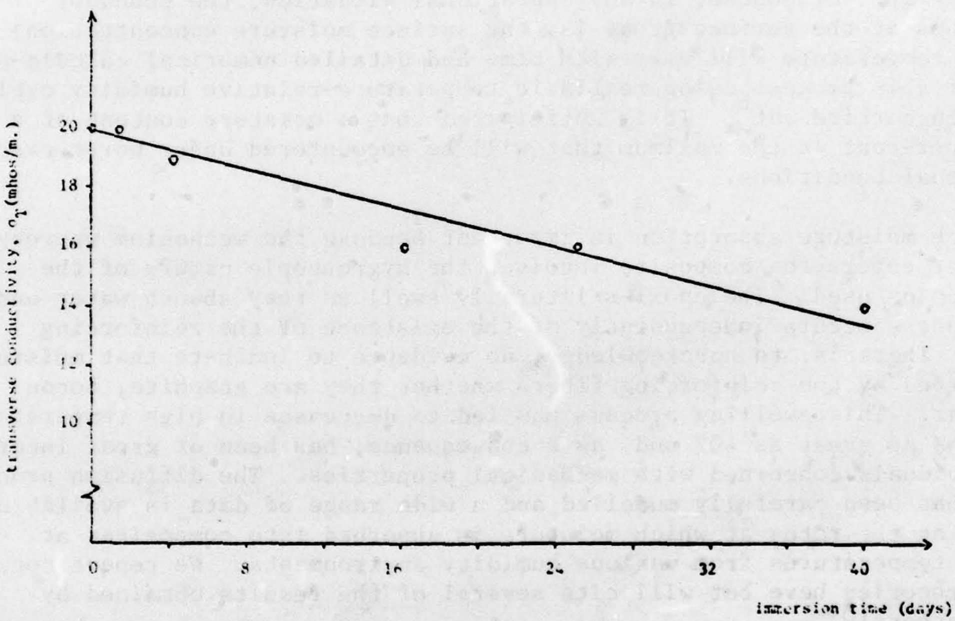

EFFECTS OF MOISTURE ON TRANSVERSE CONDUCTIVITY

FIGURE 7

It had been argued previously[3] that the transverse conductivity in graphite/epoxy depends on the degree of fiber-to-fiber contact. Theoretical analysis of composite models using triangular and hexagonal fibers had resulted in a relationship between transverse conductivity and fiber volume fraction f as sketched in Figure 8. The system displays a marked percolation; i.e., a threshold value of f below which the transverse conductivity is essentially zero. We have not yet produced samples with suitably low volume fractions to display this phenomenon but our models indicate that the percolation limit is around a volume fraction of 0.4. The theory does not apply to boron/epoxy because the boron fibers do not touch significantly.

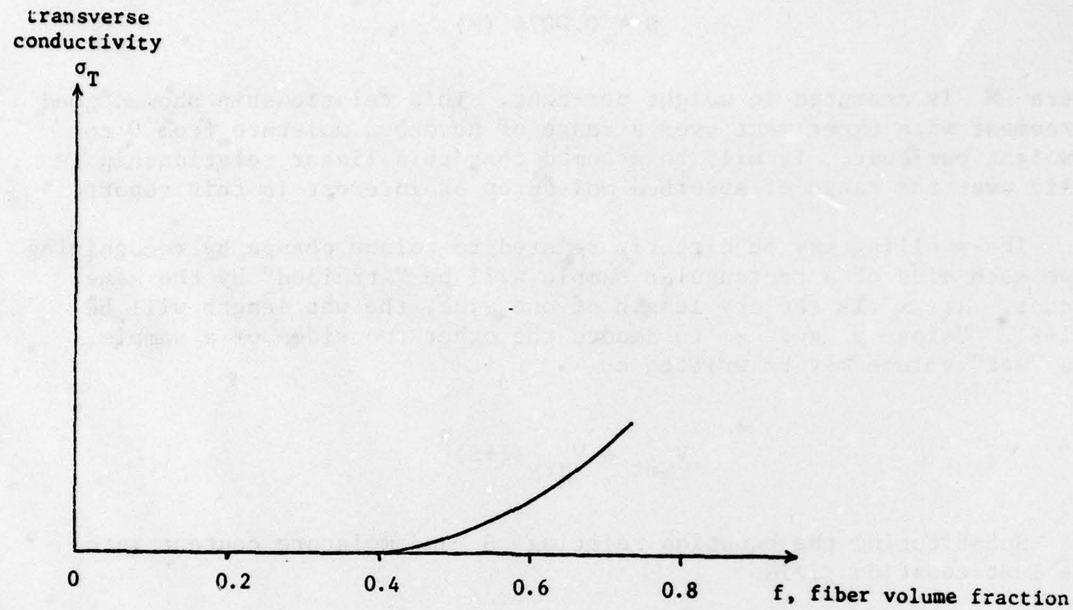

TRANSVERSE CONDUCTIVITY VS. FIBER VOLUME FRACTION

FIGURE 8

Samples have been made with volume fractions between 0.5 and 0.75 and we have found that the transverse conductivity varies with volume fraction approximately as f^5. This result is in agreement with the theoretical models over this range of volume fraction.

The effects of absorbed moisture in decreasing the transverse conductivity can be reasonably well understood in terms of this model if one recognizes that the major effect of the absorbed moisture is a swelling of the epoxy and an associated decrease in the fiber volume fraction f. As pointed out by Shirrell[11], there is no experimental evidence that the moisture is absorbed by the graphite fibers themselves. Studies of moisture absorption on both graphite/epoxy composites and epoxy samples indicate that the moisture is absorbed by the epoxy.

A simple model of this swelling has been formulated based on the assumption of additivity of volumes, that is, the swollen volume of the sample is simply the volume of the dry laminate plus the volume of the absorbed moisture. Using this assumption, Shirell[11] was able to derive a relationship between the swelling S of a sample (essentially a linear strain, measured in units of in/in) and the moisture content (M) which can be summarized as

$$S = 0.0074\ (M)$$

where M is measured in weight per-cent. This relationship showed good agreement with experiment over a range of absorbed moisture from 0 to 2 weight per-cent. It will be assumed that this linear relationship is valid over the range of absorbed moistures of interest in this report.

The swelling may be directly related to volume change by recognizing that each side of a rectangular sample will be "strained" by the same amount. If x is the dry length of one side, the wet length will be x(1+S). Using y and z to denote the other two sides of a sample, the "wet" volume may be written as

$$V_{wet} = V_{dry}(1+S)^3$$

Substituting the equation relating S and moisture content into the last equation yields

$$V_{wet} = V_{dry}(1+.0074\ M)^3$$

The total fiber volume does not, of course, change through the moisture absorbing process and, as a consequence, we may express the wet fiber volume fraction as

$$f_{wet} = \frac{V_{fibers}}{V_{wet}} = \frac{f_{dry}}{(1 + 0.0074\ M)^3}$$

Using the approximation that the transverse conductivity varies in direct proportion to the fifth power of the fiber volume fraction, the expression for the conductivity as a function of the moisture content may be written as

$$\sigma_{T,wet} = \sigma_{T,dry}(f_{wet}/f_{dry})^5$$

or

$$\frac{\sigma_{T,wet}}{\sigma_{T,dry}} = (1 + .0074\ M)^{-15}$$

Although the dependence shown in the above equation appears unlikely, it must be recognized that the moisture content is expressed as a percentage and has, as a practical matter, a maximum value on the order of 4 weight per-cent. Using published data, estimates were made of the moisture content of the unidirectional samples soaked in water for various lengths of time. Although it would have been desirable to measure the moisture content by a direct measurement of weight gain, there was not sufficient time for such efforts. The moisture contents of six samples are given in Table VI.

TABLE VI

Moisture Content (weight-%)	Theory $\sigma_{T,wet}/\sigma_{T,dry}$	Experiment $\sigma_{T,wet}/\sigma_{T,dry}$	$\sigma_{T,wet}$ (mhos/m.)
0.0	1	1	20
0.4	0.96	1	20
0.9	0.91	0.95	19
1.3	0.87	0.80	16
1.6	0.84	0.80	16
1.9	0.81	0.70	14

EFFECTS OF MOISTURE ABSORPTION ON THE TRANSVERSE CONDUCTIVITY OF GRAPHITE/EPOXY

It should be noted that each of these samples was cut from the same cured laminate and the control sample (indicated as zero moisture content) was kept in a dessicator except when its conductivity was being measured. Both theoretical and experimental plots of transverse conductivity versus absorbed moisture content are shown in Figure 9 which reveals good agreement.

As long as volume fractions remain around 0.6, it may be expected that the transverse conductivity in graphite/epoxy materials will remain relatively large although degradation on the order of 20% is to be expected under exposure to high humidity environments. This transverse conductivity is of more than academic interest because it provides the paths whereby injected charge (for example, that associated with a lightning discharge) is conducted into the interior of a composite material. If this conductivity were zero, it is expected that graphite/epoxy materials would be more susceptible to lightning than they are at the present time. These comments do not apply, of course, to protection schemes in which metallic surface coatings are used to prevent charge injection into the interior of a composite. Additional experiments need to be done but these preliminary results indicate that moisture absorption

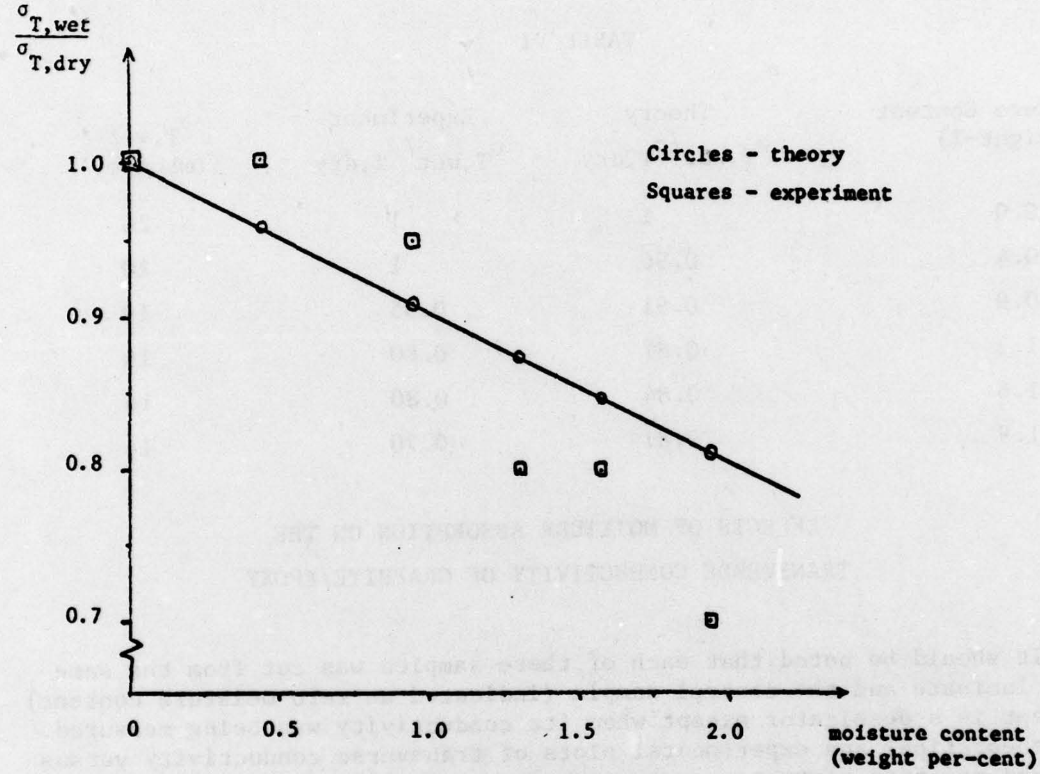

MOISTURE ABSORPTION EFFECTS COMPARISON BETWEEN THEORY AND EXPERIMENT

FIGURE 9

will have a relatively small impact on the electromagnetic properties of advanced composite materials. In the case of Kevlar/epoxy and boron/epoxy, no effects were observed while the transverse conductivity of graphite/epoxy was degraded by at most 20% upon the absorption of moisture.

6) CONDUCTANCE OF MULTIPLE-PLY SAMPLES

In calculating the effective conductance or conductivity of a multiple-ply sample, the basic assumption was made that the individual plies could be treated as conductances in parallel[1]. The germane equations are summarized in the following paragraphs.

Defining G_i as the conductance of the i^{th} layer in the direction of interest, the sample conductance G may be written as a simple summation

$$G = \sum_{i=1}^{N} G_i .$$

where N is the number of plies.

The sample has a length L, a uniform width W and each ply has a thickness Δ. The quantity G_i may then be written

$$G_i = \frac{\sigma_i W \Delta}{L}$$

where σ_i is the conductivity associated with the i^{th} layer. The total sample conductance may be expressed in terms of effective conductivity by the equation

$$G = \frac{\sigma_e A}{L} = \sum_{i=1}^{N} \frac{\sigma_i W \Delta}{L}$$

where the total sample area A has been set equal to WN. Upon cancelling common terms, it is found that

$$\sigma_e = \frac{1}{N} \sum_{i=1}^{N} \sigma_i .$$

It is essential to recognize that this derivation assumes that all plies have identical thicknesses. With this result, the effective conductivity of any multiple-ply sample can be calculated as long as the values of conductivity to be associated with the angular orientations of individual plies are known.

In using the last equation to predict values of conductivity for multiple-ply samples, it is necessary that numerical values be assigned to conductivities of single plies for the three geometries of interest: longitudinal (in which the current is along the fiber axis), transverse (in which the current is at right angles to the fiber axis) and 45° (in which the current density vector makes an angle of 45 degrees with the fiber axis). The values for the first two situations were found by direct experimentation to be approximately $1.0(10^4)$ mhos/m. and 100 mhos/m. respectively. A value of $0.5\ (10^4)$ mhos/m. was chosen for the 45° case to provide a reasonable fit to the experimental data available[1].

Table VII lists lay-up configurations as well as experimental and calculated values for conductivities.

	Lay-up	MEASURED CONDUCTIVITY (mhos/m.)	THEORETICAL CONDUCTIVITY (mhos/m.)
1.	$[0\ \underline{90}]_S$	3000	3333
2.	$[\underline{0}\ 90]_S$	7000	6667
3.	$[\underline{0}\ 45\ 90]_S$	5000	6040
4.	$[0\ 45\ \underline{90}]_S$	1700	1250
5.	$[\underline{0}\ \pm 45\ 90]_S$	8000	10000
6.	$[0\ \pm 45\ \underline{90}]_S$	2500	4300*
7.	$[\underline{0}\ \pm 45\ \underline{0}\ 90]_S$	5333	6667
8.	$[0\ \pm 45\ 0\ \underline{90}]_S$	1540	3333*
9.	$[0\ \pm 45\ 0\ \underline{90}\ \underline{90}]_S$	2500	4545*
10.	$[\underline{0}\ \pm 45\ \underline{0}\ 90\ 90]_S$	5000	5454
11.	$[0\ \underline{90}\ \pm 45\ \pm 45\ \underline{90}\ 0]_S$	5000	5300
12.	$[\underline{0}\ 90\ \pm 45\ \pm 45\ 90\ \underline{0}]_S$	2500	4667

TABLE VII

INDEPENDENT PLY ASSUMPTION COMPARED TO EXPERIMENT

The underscore in each lay-up configuration denotes the direction of current which produced the measured value of conductivity indicated. In addition, an asterisk has been placed on each line in which the theoretical value of conductivity differed significantly (by more than 70%) from the measured value.

As mentioned above, a value had been assigned to the 45° conductivity by the fit to the available data. In order to explain the puzzling discrepancies in the above table, a set of samples were constructed so that the fibers ran at a 45° angle between opposite faces. The samples were unidirectional. The measured conductivities were on the order of 20 mhos/m. - a very different value from that used to theoretically determine conductivities of multiple-ply samples. Upon reflection, it is clear that the conductivity of such samples must be small as long as the individual fibers do not reach from one electrode face to the other. This was the situation in all our measurements. Sample sizes had length to width aspect ratios of at least three and, in many cases, 10 to 20. In such cases, charge flow must be controlled by fiber-to-fiber contact and the measured conductivity will be correspondingly low.

When this reasoning is accepted, the problem appears to worsen because the fit between experiment and theory in the above table becomes even worse if all 45° plies are assumed to have negligible conductance.

The resolution of this dilemma lies in a recognition that the plies are not electrically independent of each other but rather are in contact. A detailed model is not possible but we note one significant fact. In experimental situations in which the 45° layers are sandwiched between layers transverse to the direction of charge flow, it is to be expected that their overall contribution to sample conductivity will be essentially zero. Table VIII indicates recalculated values for samples 6, 8, 9 and 12 in which 45° layers are isolated in this way. The column labeled revised theory contains values calculated by assuming that the 45° layers have essentially zero conductivity. With this change, the calculated values of conductivity are all within 70% of the measured values.

It is clear from these arguments that one may not simply assume that the layers in a multiple-ply composite sample are electrically independent of each other under low-frequency excitations. There is a physical and electrical coupling between these layers which must be more accurately modelled if valid predictions of conductivity are to be made.

CONDUCTIVITIES (mhos/m.)

Sample	Measured	Initial Theory	Revised Theory
6	2500	4300	1430
8	1540	3333	1111
9	2500	4545	2727
12	2500	4667	2000

TABLE VIII

EFFECTS OF PLY DEPENDENCE INCLUDED

7) CONCLUSIONS AND SUMMARY

Simple measurement techniques may be used to characterize composite materials over the frequency range from DC to 50 MHz. The magnetic properties of these materials may be measured by sample weighing methods or a vibrating sample magnetometer. All three materials of interest were found to be weakly diagmagnetic. The relative permeability of these materials is unity to within one part in ten million.

Kevlar/epoxy is electrically isotropic and is a good dielectric. The conductivity is on the order of 10^{-9} mhos/m. while the relative permittivity varies between 3.6 and 5.8. Boron/epoxy has a transverse conductivity of $2(10^{-8})$ mhos/m. and a longitudinal conductivity on the order of 1000 mhos/m. Care must be taken to make low resistance electrical contacts to the highly conductive cores of the boron fibers. The only method found suitable in the course of this research involved nickel plating.

Graphite/epoxy may be considered to be a good conductor with an anisotropy ratio on the order of 200. Although the impedance of a graphite/epoxy sample increases with frequency in the range from 5 to 50 MHz, a coupled circuit theory model has been developed to explain this phenomena in terms of the inductive coupling between fibers and the intrinsic electrical conductivity remains constant over this range of frequencies.

Absorbed moisture has no effect on electrical conductivities of Kevlar/epoxy or boron/epoxy. Nor is the longitudinal conductivity of graphite/epoxy affected by moisture. The transverse conductivity of graphite/epoxy does show a relatively small decrease as moisture is absorbed but it is unlikely that this will be operationally significant as long as the volume fractions of fibers remain above 0.4.

8) ACKNOWLEDGEMENTS

P.K. Ajmera, L.A. Scruggs and M. McGillan contributed to this research through measurements of composite conductivities and formulation of the coupled circuit theory model.

W. Strieder and T. Joy formulated the models of transverse conductivity cited in section 4.

R. Kwor and C. Araujo provided the electrical characteristics of boron fibers.

Helpful technical discussions with J.L. Allen (University of South Florida), R. Heintz and W.F. Walker (Rochester Institute of Technology) and R. Stratton (RADC) are gratefully acknowledged.

The assistance of D. Shirrell and R. Achard (Wright-Patterson Air Force Base) in fabricating composite samples is also appreciated.

REFERENCES

1. J.L. Allen et al, Electromagnetic Properties and Effects of Advanced Composite Materials: Measurement and Modeling, RADC-TR-78-156, June, 1978, A058041.

2. C. Skouby, Electromagnetic Effects of Advanced Composites, Final Report (ONR), Contract N00014-74-C-0200, January, 1975.

3. W.J. Gajda, Jr., A Fundamental Study of the Electromagnetic Properties of Advanced Composite Materials, RADC-TR-78-158, July, 1978, A059029.

4. D. Kim et al, Measurement of Advanced Composite Shielding Effectiveness, AFFDL-TR-74-30, 1974.

5. Ramo, Whinnery and Von Duzer, Fields and Waves in Communication Electronics, J. Wiley, 1965.

6. P. Graneau, Alternating and Transient Conduction Currents in Straight Conductors of any Cross-Section, International J. Electronics 19 p. 41-59 (1965).

7. H. Dwight, Effective Resistance of Isolated Nonmagnetic Rectangular Conductors, AIEE Transactions, 68, p. 549-552 (1947).

8. H. Forbes and L. Gorman, Skin Effect in Rectangular Conductors, AIEE Transactions, 54, p. 516-519 (1933).

9. J. Hertz, High Temperature Strength Degradation of Advanced Composites, S.A.M.P.E., Vol. 3, p. 9-16 (1970).

10. E. McKague et al, Moisture Diffusion in Fiber Reinforced Plastics, Trans. ASME, p. 92-95 (1976).

11. D.C. Shirrell and J. Halpin, Moisture Absorption and Desorption in Energy Composite Laminates, ASTM STP 617, p. 514-528, (1977).

APPENDIX A

EXPLANATION OF PROGRAM I

Lines 1 to 15 are used to define necessary arrays and constants. Some of these are listed below while others will be explained later in the discussion of the program.

LE: Denotes the number of "C" coefficients to be calculated for each fiber (this index does not include $C_1 = 1/R$).

II: Denotes the number of fibers on each side of the square sample.

ZL: Denotes the length of the sample in meters.

DFIB: Denotes the nearest neighbor distance between fibers in meters.

II2: Denotes the number of fibers in a sample.

Lines 16 and 17 establish a numbering system for the fibers as illustrated in Figure 4.

In lines 18 and 20, the distance between fiber (1,1) and every other fiber in the sample is determined. These distances are stored in the array ZZM(J,K) where a given element is the distance, in meters, between fiber (1,1) and fiber (J,K).

In lines 21-22, the values of the array ZZM are replaced with the applicable mutual inductances. This is done using the solution of Neumanns' formula described earlier. These values are then printed by the execution of line 23. In line 25, the self inductance of a fiber is set to zero. This is equivalent to placing zeros along the diagonal of the mutual inductance matrix. This can be done because the fibers are assumed to be vanishingly thin.

In lines 28 to 44, the C_i coefficients are calculated using the procedures described above. Two properties of the sample and the inductance matrix are used to shorten the execution time of the program. First, since the mutual inductance is a function of the length of the sample and the distance between the fibers and because each fiber has the same length, only the distance between the fibers concerned needs to be calculated. An examination of Figure 4 reveals that every possible fiber-to-fiber distance is included in the set of distances between fiber (1,1) and all of the other fibers. Plus every possible mutual inductance is contained in the set of mutual inductances between the first fiber and the other fibers. These values are stored in the array ZZM (J,K).

The loops in this part of the program generate the necessary set of distances and then carry out the calculations of the C coefficients described in the narrative of the report. The above process continues until all of the rows in the mutual inductance matrix have been added. At this point, the fact that $M_{nm} = M_{mn}$ implies that corresponding rows and columns of the matrix will be identical. Hence, the sums of the elements of these rows and columns will be equal and this is used in completing the summation of the products in line 44. It will be noted that in this line the value of C(L3,J2) changes from 1 to the value of the elements in row a and then to the value of the elements in row b and continues this until all the desired values ($R_f^2C_2$, $R_f^3C_3$...) for each fiber have been stored in the array C .

In lines 45 to 56, the numbering of the fibers is changed again to facilitate subsequent calculations. We shall not describe this process in detail since it is of interest only to an individual trying to re-write or modify the program.

In lines 57-80, the real and reactive currents flowing in each fiber are determined using the power series expansion developed in the coupled circuit theory. The values stored in the arrays CURR and REAC are the real and reactive components of the current in fiber J at a frequency of L MHz. The values of these currents at the points indicated in Figure 6 are printed by the execution of lines 82 and 83.

The remainder of the program calculates and prints, in an obvious way, the impedance of the sample as a function of frequency.

```
1           DIMENSION FREQ(30),RTZ(30)
            DIMENSION CURR(30,200),REAC(30,200)
            DIMENSION ZZM(40,40)
            DIMENSION C(10,1600)
            IF=30
            LE=6
            LE1=LE+1
            LE2=LE/2
            II=40
            IL=.07
11          DFIB=7.98E-6
            II2=II**2
            II22=II/2
            II24=II2/4
            II28=II2/8
            DO 1 J=1,II
            DO 1 K=1,II
            ZZM(J,K)=SQRT(FLOAT((J-1)**2+(K-1)**2))
            IF (ZZM(J,K) .LE. 0.) GO TO 1
            ZZM(J,K)=DFIB*ZZM(J,K)
21           ZZM(J,K)=2.*(ZL*ALOG((ZL+SQRT(ZL**2+ZZM(J,K)**2))/
           $ZZM(J,K))
           $ -SQRT(ZL*
           $*2+ZZM(J,K)**2)+ZZM(J,K))
```

```
      ZZM(J,K)=ZZM(J,K)*(1.E-7)
      WRITE(6,*) J,K,ZZM(J,K)
1     CONTINUE
      ZZM(1,1)=0
      DO 8 J2=1,II2
8     C(1,J2)=1.
      DO 9 L2=2,LE1
      J1=0
      DO 9 J=1,II
      DO 9 K=1,II
      J1=J1+1
      J2=0
      DO 9 L=1,II
      DO 9 M=1,II
      J2=J2+1
      ZJL=J-L
      ZKM=K-M
      N=ABS(ZJL)
      I=ABS(ZKM)
      N=N+1
      I=I+1
      L3=L2-1
9     C(L2,J1)=C(L3,J2)*ZZM(N,I)+C(L2,J1)
      DO 10 L2=2,LE1
      DO 10 J1=1,II2
      L=L2-1
10    C(L,J1)=C(L2,J1)
      DO 20 L=1,IF
      J1=0
      DO 20 I=1,II22
      K=(I-1)*II+I
      M=K+(II22-I)
      DO 20 J=K,M
      J1=J1+1
20    C(L,J1)=C(L,J)
      R1=67942.0
      DO 65 L=1,LE
      M=L+1
      DO 65 J=1,II28
65    C(L,J)=C(L,J)/(R1**M)
      FREQZ=1.E6
      TPI=2.*3.14159
      FREQ(1)=FREQZ
      DO 70 L=2,IF
      M=L-1
70    FREQ(L)=FREQZ+FREQ(M)
      DO 75 J=1,II28
      DO 75 L=1,IF
      CURR(L,J)=0.
      REAC(L,J)=0.
      DO 75 K=1,LE2
```

```
                  M=2*K
                  CURR(L,J)=((-1.)**K)*C(M,J)*((FREQ(L)*TPI)**M)+
                 $CURR(L,J)
                  N=2*K-1
                  REAC(L,J)=((-1.)**K)*C(N,J)*((FREQ(L)*TPI)**N)+
                 $REAC(L,J)
            75    CONTINUE
                  DO 80 J=1,II28
                  DO 80 L=1,IF
            80    CURR(L,J)=CURR(L,J)+(L./R1)
 81               DO 81 L=1,IF
                  WRITE (6,*) CURR(L,1),CURR(L,II22),CURR(L,II28)
            81    WRITE (6,*) REAC(L,1),REAC(L,II22),REAC(L,II28)
                  DO 82 J=1,II28
                  DO 82 L=1,IF
            82    CURR(L,J)+SQRT(CURR(L,J)**2+REAC(L,J)**2)
                  DO83 L=1,IF
            83    WRITE (6,*) CURR(L,1),CURR(L,II22),CURR(L,II28)
                  DO 85 K=1,II28
                  DO 85 L=1,IF
 91         85    CURR(L,K)=1./(CURR(L,K)*8.)
                  DO 100 L=1,IF
                  RTZ(L)=0.
                  DO 90 J=1,II28
            90    RTZ(L)=1./CURR(L,J)+RTZ(L)
           100    RTZ(L)=1./RTZ(L)
                  DO 91 L=1,IF
            91    WRITE(6,*) FREQ(L),RTZ(L)
                  C(L,2)=C(L,II22)
                  C(L,3)=C(L,II24)
101               DO 105 L=1,LE
           105     WRITE(6,*) (C(L,J),J=1,3)
                  STOP
                  END
```

EXPLANATION OF PROGRAM II

This program calculates approximate impedances of the graphite samples and is not as accurate as Program I. However, in situations in which comparison was possible, the impedances given by this program were within 10% of those produced by Program I. This approximation was developed after a careful examination of the numerical results from the first program when it was found that the inductance coefficients across the entire sample did not vary by more than a ratio of 2:1 for a 40 x 40 sample. This resulted in an even smaller variation of the coefficients. In program II, the coefficients were calculated only for the fiber indicated in Figure 6. The coefficients for this fiber being an average of all the other fibers in the matrix were all the same. This results in a smearing out of the overall mutual inductive coupling in the sample.

That the results of the impedance calculations from both programs were so similar indicates that the impedance increase observed in graphite/epoxy is primarily due to inductive reactance and not a redistribution of the current as in the skin effect. This is so because giving each fiber the same coefficients meant that the current distribution over the samples cross-section was forced to be uniform.

Program II is quite similar to Program I. For this reason, only the differences in the two programs will be outlined here. Since uniformity has been assumed, the CURR, REAC and C arrays will consist only of single elements. In lines 110 to 185, the inductance coefficients between each fiber and the fiber for which the coefficients are to be found are calculated. These inductances are added in line 186 to produce $R_f{}^2C_2$ for this fiber. If it is assumed that all rows in the inductance matrix have elements which add to give the same value of this factor, then $R_f{}^iC_i$ can be found using the formula

$$R_f{}^iC_i = (R_f{}^2C_2)^{i-1}$$

The rest of the program is essentially identical to the first version.

```
10        DIMENSION FREQ(30),RTZ(30)
15        DIMENSION AVE(50)
20        DIMENSION CURR(30,3),REAC(30,3)
40        DIMENSION C(10,1)
41        IF=30
42        LE=6
43        LE1=LE+1
44        LE2=LE/2
50        II=100
60        ZL=.082
70        DFIB=7.98E-6
80        II2=II**2
```

```
      II22=II/2
      II24=II2/4
      II28=II2/8
      ZII2=FLOAT(II2)
      D=0.
      DO 1 J=1,II
      DO 1 K=1,II
      ZZM=SQRT(FLOAT((J-1)**2+(K-II22)**2))
      IF (ZZM .LE. 0.) GO TO 1
      ZZM=DFIB*ZZM
       ZZM=2.*(ZL*ALOG((ZL+SQRT(ZL**2+ZZM**2))/ZZM)
      $ -SQRT(ZL*
      $*2+ZZM**2)+ZZM)
      ZZM=ZZM*(1.E-7)
      D=ZZM+D
    1 CONTINUE
      C(1,1)=D
      DO 4 L=1,LE
      C(L,1)=C(1,1)**L
    4 WRITE(6,*) C(L,1)
      R1=214628.
      DO 65 L=1,LE
      M=L+1
      J=1
   65 C(L,J)=C(L,J)/(R1**M)
      FREQZ=1.E6
      TPI=2.*3.14159
      FREQ(1)=FREQZ
      DO 70 L=2,IF
      M=L-1
   70 FREQ(L)=FREQZ+FREQ(M)
      J=1
      DO 75 L=1,IF
      CURR(L,J)=0
      REAC(L,J)=0
      DO 75 K=1,LE2
      M=2*K
      CURR(L,J)=((-1.)**K)*C(M,J)*((FREQ(L)*TPI)**M)+
     $CURR(L,J)
      N=2*K-1
      REAC(L,J)=((-1.)**K)*C(N,J)*((FREQ(L)*TPI)**N)+
     $REAC(L,J)
   75 CONTINUE
      DO 80 L=1,IF
   80 CURR(L,J)=CURR(L,J)+(1./R1)
      DO 81 L=1,IF
      WRITE (6,*) CURR(L,1)
   81 WRITE (6,*) REAC(L,1)
      DO 82 L=1,IF
   82 CURR(L,J)=SQRT(CURR(L,J)**2+REAC(L,J)**2)
      DO 83 L=1,IF
   83 WRITE (6,*) CURR(L,1)
```

```
      DO 110 L=1,IF
110   AVE(L)=1./(ZII2*CURR(L,J))
      DO 115 L=1,IF
115   WRITE (6,*) FREQ(L),AVE(L)
      DO 116 L=1,LE
116   WRITE(6,*) C(L,J)
      STOP
      END
```

MISSION
of
Rome Air Development Center

RADC plans and executes research, development, test and selected acquisition programs in support of Command, Control Communications and Intelligence (C^3I) activities. Technical and engineering support within areas of technical competence is provided to ESD Program Offices (POs) and other ESD elements. The principal technical mission areas are communications, electromagnetic guidance and control, surveillance of ground and aerospace objects, intelligence data collection and handling, information system technology, ionospheric propagation, solid state sciences, microwave physics and electronic reliability, maintainability and compatibility.